

TURBO CODED BURST BY BURST ADAPTIVE WIDEBAND MODULATION WITH BLIND MODEM MODE DETECTION

C. H. Wong, T. H. Liew and L. Hanzo

Dept. of Electronics and Computer Science,
University of Southampton, SO17 1BJ, UK.

Tel: +44-703-593 125, Fax: +44-703-594 508

Email: lh@ecs.soton.ac.uk

<http://www-mobile.ecs.soton.ac.uk>

ABSTRACT

Adaptive modulation is applied in conjunction with a Decision Feedback Equalizer (DFE) in order to mitigate the effects of the slowly varying wideband multi-path Rayleigh fading channel in a noise-limited environment. Turbo BCH coding was applied in order to improve the BER and BPS performance and subsequently, the Soft-Decision (SD) based error detection capability of the turbo codec was utilized by the proposed blind modulation detection algorithm in order to detect the various modulation modes.

1. INTRODUCTION

Adaptive Quadrature Amplitude Modulation (AQAM) is employed in order to maximise the throughput as well as providing a more error resilient system. This is achieved by utilizing a higher-capacity modulation mode when the channel is favourable and conversely, a more robust lower order modulation level when the channel exhibits a deep fade. In a narrow-band channel environment, AQAM was applied by amongst others, Webb and Steele[1], Sampei *et al*[3] and Torrance *et al* [2]. This adaptive system can be conveniently implemented in an Time Division Duplex (TDD) environment where the channel is slowly varying and reciprocal in nature.

When applying AQAM in a wideband channel environment, the equalization process will eliminate most of the intersymbol interference (ISI) and imposing a Gaussian-like noise plus interference distribution on the signal. Consequently, this impairment can be approximated by a Gaussian distribution process of an increased variance which can be quantified in terms of the associated SNR at the output of the DFE, which can be used as a criterion to switch modulation modes. This ensures that the performance is optimised by employing equalization and AQAM techniques to combat signal power fluctuations and ISI in a wideband channel. Furthermore, the error correction and the SD-based error detection capability of the turbo BCH codec employed is exploited, in order to improve the BER and throughput performance. Recent work on combining channel coding with AQAM has been carried out by Matsuoka *et al* [4] where punctured convolutional coding with and without an outer Reed Solomon (RS) outer code was invoked in a TDD environment. Convolutional coding was also used in conjunction with AQAM in Reference [5] where results were presented related to both a FDMA and TDMA environment while assuming a feedback path between the receiver and transmitter. Finally, coset codes based AQAM was also advocated by Goldsmith *et al* [6].

2. SYSTEM OVERVIEW

At the receiver, the DFE coefficients can be calculated using Equations proposed in Reference [7]. Additionally, the instantaneous channel quality estimates and the DFE coefficients are utilized to compute the estimated output SNR of the DFE termed as the pseudo-SNR, γ_{dfc} . By assuming that the residual ISI is Gaussian distributed and that decision feedback errors can be neglected, the pseudo-SNR at the output of the DFE, γ_{dfc} can be calculated as [8]:

$$\gamma_{dfc} = \frac{E\left[|S_k \sum_{m=0}^{N_f} C_m h_m|^2\right]}{\sum_{q=-(N_f-1)}^{-1} E\left[\left|\sum_{m=0}^{N_f-1} C_m h_{m+q} S_{k-q}\right|^2\right] + N_o \sum_{m=0}^{N_f} |C_m|^2}, \quad (1)$$

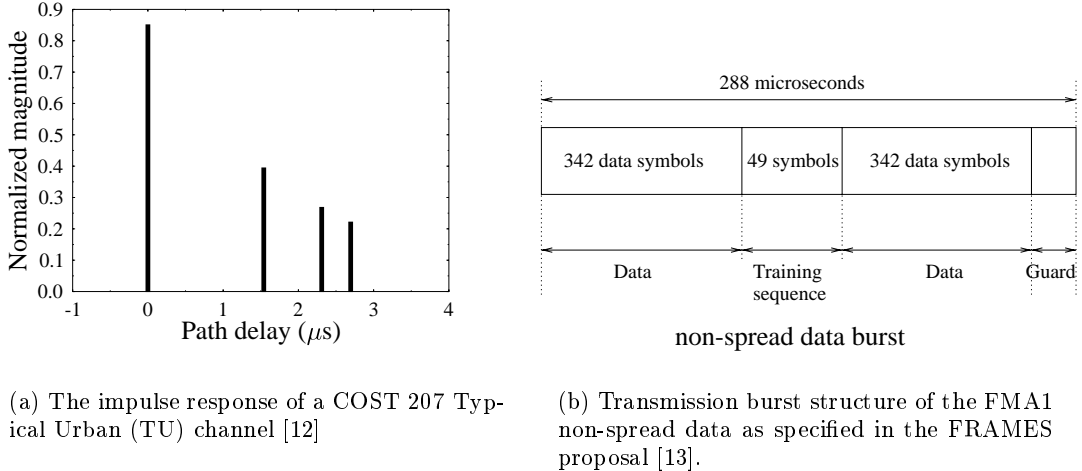


Figure 1: The channel impulse response and the transmission burst structure.

where C_m and h_m denotes the DFE feed-forward coefficients and the channel impulse response taps, respectively. The transmitted signal and the noise spectral density are represented by S_k and N_o . Lastly, the number of DFE feed-forward coefficients is denoted by N_f .

The pseudo-SNR is then compared to a set of pseudo-SNR thresholds, f_n and a modulation scheme is selected for the next transmission burst according to the regime of Table 1. The NOTX mode listed in Table 1 is used to temporarily disable transmission under severely degraded instantaneous channel conditions. Furthermore, the selected modulation mode is also used to select the turbo interleaver size according to Table 1.

Turbo coding is a form of iterative channel decoding technique, which was introduced by Berrou *et al* [9]. In the AQAM system, in order to maximise the throughput of the system, high code rates in excess of $\frac{2}{3}$ are desirable. Consequently, block codes were chosen as the component codes in preference to Recursive Systematic Convolutional (RSC) codes since turbo block coding has generally shown better results for coding rates above $\frac{2}{3}$ [10]. The BCH (31, 26) code is used as the component code with the number of turbo coding iterations set to six. The Log-MAP decoding algorithm [11] was utilized and the random turbo interleaver size was varied according to the modulation mode selected as shown in Table 1. A random turbo interleaver size was chosen in order to ensure burst-by-burst decoding and subsequently we were able to exploit the SD-based error correction capability to detect the modulation mode used, an issue which will be discussed in Section 4.

The multi-path channel model is characterized by its discretised symbol-spaced COST207 Typical Urban (TU) channel impulse response [12], as shown in Figure 1(a). Each path is faded independently according to a Rayleigh distribution and the corresponding normalised Doppler frequency is 3.27×10^{-5} . The DFE incorporated 35 feed-forward taps and 7 feedback taps and the transmission burst structure used for our treatise is shown in Figure 1(b). For the scope of our paper, perfect channel estimation and initially also perfect modulation selection was utilized.

	$\gamma_{dfe} < f_1$	$f_1 \leq \gamma_{dfe} < f_2$	$f_2 \leq \gamma_{dfe} < f_3$	$f_3 \leq \gamma_{dfe} < f_4$	$\gamma_{dfe} \geq f_4$
Mod. Mode	NOTX	BPSK	4QAM	16QAM	64QAM
Turbo Interleaver Size	-	494	988	1976	2964

Table 1: The modulation switching mechanism based on the pseudo-SNR, γ_{dfe} , and the switching thresholds, $f_n, n = 1, 2, 3, 4$ for the AQAM system. The corresponding turbo coding interleaver size is also shown for each modulation mode, where a random turbo interleaver algorithm was used.

3. TURBO CODED AQAM PERFORMANCE

The associated BER and BPS performances are shown in Figure 2, where the channel coded system's switching thresholds are set according to Table 2. Due to the analytically intractable non-linear channel coding characteristics, the switching thresholds were not optimised. However, these thresholds were adjusted intuitively, in

order to obtain a BER performance of below 0.01% as well as to create an error free system. Their performances were then compared to the uncoded AQAM system, where the uncoded switching thresholds were optimised using a method similar to that introduced by Torrance *et al* [14] in order to achieve a target BER 0.01%, as shown in Table 2. Referring to Figure 2(a), the coded BPS was higher than that of the uncoded scheme for the channel SNR range of 0 to 22dB, exhibiting a maximum BPS gain of 6dB at a channel SNR of 0dB. The coded AQAM system also displayed a superior BER performance, when compared to the uncoded system where a BER reduction of nearly two orders of magnitude was observed at a channel SNR of 20dB.

Target BER	Switching Thresholds			
	f_1	f_2	f_3	f_4
Uncoded $\leq 1\%$	3.63628	6.2258	11.6450	17.6846
Uncoded $\leq 0.01\%$	8.30459	10.4541	16.8846	23.051
Coded $\leq 0.01\%$	1.9958	4.2079	10.5480	17.5089
Error Free	3.2458	5.4579	11.7980	18.7589

Table 2: The coded switching thresholds which were intuitively set to achieve the target BER of below 0.01% as well as to create an error free turbo coded AQAM system. The switching mechanism was characterized by Table 1 and the uncoded switching thresholds were optimised in order to achieve the target BER of 1% and 0.01%[14].

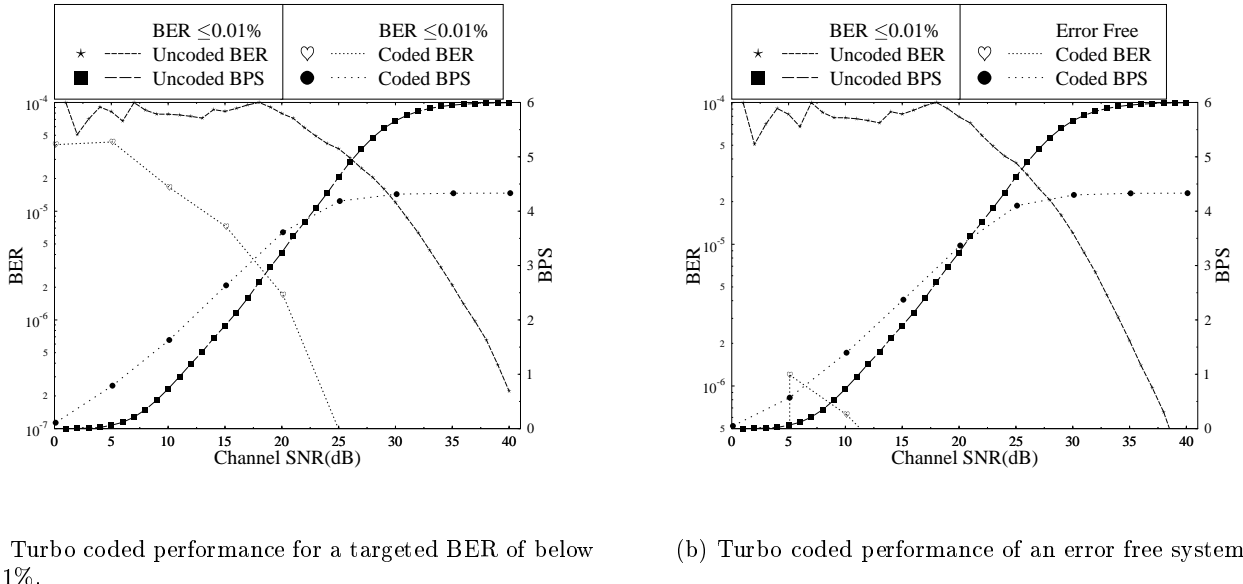


Figure 2: Turbo coded performance of the AQAM system where the generic system parameters were described in Section 2. The coded switching methodology and the variable random turbo interleaver size was characterized by Table 1. The coded and uncoded AQAM switching thresholds were set according to Table 2 for a target BER of 0.01% and the transmission burst structure of Figure 1(b) was utilized.

The BPS performance for the error free coded system was better, than that of the uncoded AQAM system for the channel SNR range of 0 to 20dB, as evidenced by Figure 2(b). However at high channel SNRs, the BPS performance was limited by the coding rate of the system to a maximum BPS of 4.33.

4. CODING BASED MODULATION DETECTION ALGORITHM

Since this coded AQAM system employed burst-by-burst decoding at the receiver, we can exploit the error correction capability of the channel codec in order to detect the modulation mode that was utilized by the transmitter. This reduces the amount of signalling required between the receiver and transmitter. Before we describe the modulation mode detection algorithm, we will address the concept of transmission blocking in AQAM. Practically, whenever the transmission is temporarily disabled due to the instantaneously low channel

quality, a transmission burst constituted by a known sequence is transmitted, which is used to estimate the channel and hence aid the selection of the next modulation mode. This burst is BPSK modulated in order to provide maximum integrity. However, at the receiver this sequence must be unique and easily identifiable which will aid the recognition of the NOTX mode. Consequently, we proposed to use the binary maximal-length shift register sequences, $C^{(a)}$, commonly known as m-sequences that exhibit the following correlation properties [15]:

$$\begin{aligned}\theta_a(0) &= Q, \\ \theta_a(r) &= -1 \quad \text{for } r \neq 0,\end{aligned}\quad (2)$$

where $\theta_a(r) = \sum_{i=0}^{Q-1} C_i^{(a)} C_{r+i}^{(a)}$ and Q is the length of the known m-sequence. Explicitly, at the transmitter, if the NOTX mode is selected, a number of copies of the same m-sequence are concatenated, in order to form the transmission burst. Consequently, at the receiver, the demodulated burst is correlated with the known m-sequence and if a maximum amplitude of Q is detected periodically, corresponding to the correlation time-shift of zero, the burst is deemed to be a NOTX mode burst.

In order to detect the BPSK, 4QAM, 16QAM and 64QAM modes, we exploited the soft input and output bit probabilities of the BCH decoder and the mean square phasor error. The mean square phasor error, defined at a later stage by Equation 4, is the Euclidean distance between the received equalized data symbols and the nearest valid constellation point for a particular AQAM mode. Specifically, we utilized the mean square phasor error to detect the BPSK mode, while the other modes were detected using the soft bit probabilities of the decoder, yielding the Soft Decision Mean Square Error (SD-MSE) modulation detection algorithm. In exploiting the soft

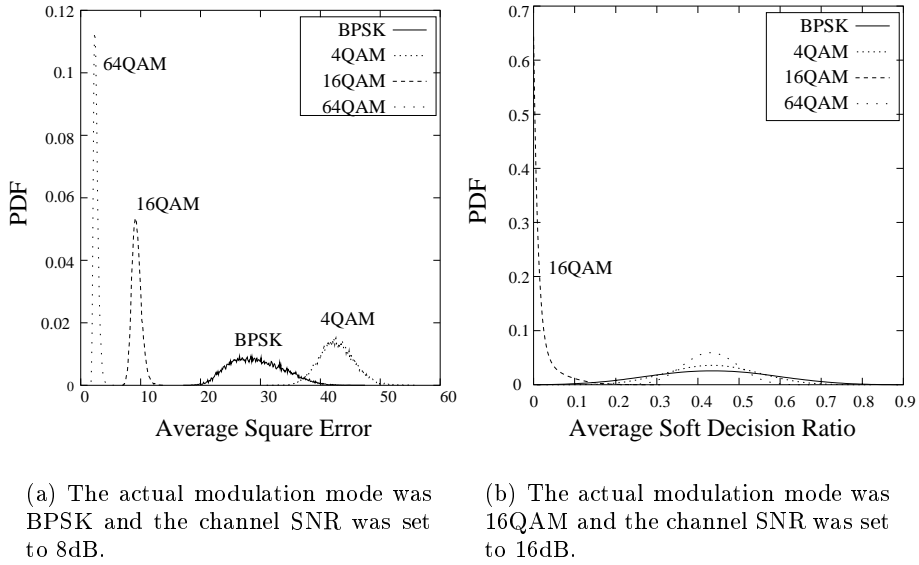


Figure 3: The PDF of the mean square phasor error and average soft decision ratio defined in Equations 4 and 5 of each individual modulation scheme for various channel SNRs.

bit probabilities of the decoder, each input bit probability entering the channel decoder was compared against its corresponding output bit probability for each possible modulation mode. The results were then classified into two categories, where one of the categories corresponded to the case, where the input bit probability was less than the output bit probability and vice-versa for the other category. These two categories were then used to update a Soft Decision counter, SD_{ratio} corresponding to the ratio of the number of occurrences in the above two categories and consequently an average SD_{ratio} was determined for all modulation modes as follows:

$$SD_{ratio}^{n,m} = \begin{cases} SD_{ratio}^{n,m} & \text{if } p_{ipbit}^{n,m} \leq p_{opbit}^{n,m} \\ SD_{ratio}^{n,m} + 1 & \text{if } p_{ipbit}^{n,m} > p_{opbit}^{n,m}, \end{cases} \quad (3)$$

$$\text{Average } SD_{ratio}^m = \frac{\sum_{n=0}^X SD_{ratio}^{n,m}}{X},$$

for $m = 4\text{QAM}, 16\text{QAM}, 64\text{QAM}$

where $p_{ipbit}^{n,m}$ represents the n th input bit probability, which was demodulated using the modulation mode, m . Similarly, $p_{opbit}^{n,m}$ denotes the output bit probability of the channel decoder and X denotes the number of coded

bits in a transmission burst. Subsequently, the final modulation mode was chosen on the basis of evaluating the mean squared phasor error given by:

$$e_q = \frac{\sum_{n=0}^Y |(R_{n,q}^{eq} - \hat{R}_{n,q})|^2}{Y} \quad \text{for } q = \text{BPSK, 4QAM} \quad (4)$$

where $R_{n,BPSK}^{eq}$ and $\hat{R}_{n,BPSK}$ are the n th equalized symbol and the corresponding de-mapped valid constellation point of the BPSK mode, e_q represents the mean square phasor error for the modulation mode, q and Y denotes the number of symbols in a transmission burst. The final decision rule is formulated as:

$$mod_c = \begin{cases} \text{BPSK} & \text{if } e_{BPSK} \leq e_{4QAM} \\ \min(\text{Average } SD_{ratio}^m) & \text{if } e_{BPSK} > e_{4QAM}, \text{for } m = 4\text{QAM, 16QAM, 64QAM} \end{cases} \quad (5)$$

where mod_c is the modulation scheme chosen and $\min(a_m)$ is the selection function that selects the minimum of all a_m values.

The PDF of the mean square phasor error, when BPSK was utilized is shown in Figure 3(a) where there was sufficient statistical separation between the PDF of the BPSK and 4QAM modes. It was this PDF separation that enabled the receiver to differentiate between the BPSK and 4QAM modes. The PDF of the average soft decision ratio, when 16QAM was transmitted is also shown in Figure 3(b). There is a clear PDF separation between the 16QAM mode and the other modulation modes, where the SD_{ratio} of the 16QAM mode is centered at the minimum end of the average SD_{ratio} scale. It was this PDF separation that ensured the feasibility to detect the different modulation modes. It must be stated that this trend was also observed, when the 4QAM and 64QAM modes were being detected.

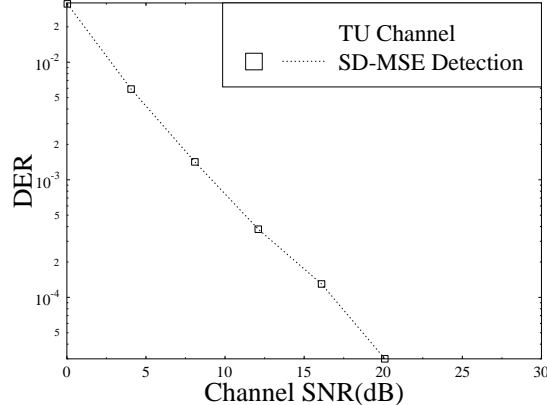


Figure 4: The modem mode detection error rate (DER) performance of the SD-MSE algorithm characterized by Equation 5. The system parameters were described in Section 2 and the AQAM switching thresholds were set according to Table 2 for the targeted BER of 1%. The DER measure was defined in Section 4 and a conventional non-iterative LOG-MAP BCH(31, 26) coding scheme was utilized.

The performance of this algorithm in terms of its modulation Detection Error Rate (DER) is depicted in Figure 4, where a conventional non-iterative LOG-MAP BCH (31, 26) decoder was used for simplicity, although this algorithm can be also readily applied to a turbo coded system. The hybrid SD-MSE algorithm achieved a DER of 10^{-4} at a channel SNR of approximately 15dB over a COST 207 TU channel. The coded switching thresholds were set for the target BER of 1% according to Table 2. This ensured that the magnitude of the switching threshold levels were lower and consequently the modulation mode switching will occur more frequently at low average channel SNRs. This will in turn highlight the robustness of the detection algorithm at low average channel SNRs. However the detection algorithm complexity increased due to the repetitive channel decoding needed for each modulation mode.

5. CONCLUSION AND FURTHER WORK

We have demonstrated the application of turbo BCH coding in conjunction with AQAM in a wideband fading channel. Specifically, we have recorded an improved coded BPS and BER performance at low to medium channel

SNRs, as evidenced by Figure 2(a). A virtually error-free turbo-coded AQAM system was also characterized in Figure 2(b). Finally, we introduced a modulation detection algorithm based on the error correction capability of the BCH code and recorded the DER performance shown in Figure 4. In our current work, we are quantifying the impact of co-channel interference and the channel estimate latency on the AQAM system.

6. ACKNOWLEDGEMENTS

The financial support of the European Union under the auspices of the Pan-European FIRST project and that of Motorola ECID, Swindon UK is gratefully acknowledged. The authors also wish to thank the members of the FIRST consortium for helpful discussions and for their friendship.

7. REFERENCES

- [1] W.T. Webb and R. Steele, "Variable Rate QAM for mobile radio," *IEEE Transactions on Communications*, vol. 43, pp. 2223 – 2230, July 1995.
- [2] J.M. Torrance and L. Hanzo, "On the Upper bound performance of adaptive QAM in a slow Rayleigh fading," *IEE Electronics Letters*, pp. 169 – 171, April 1996.
- [3] S. Sampei, S. Komaki and N. Morinaga, "Adaptive Modulation/TDMA scheme for large capacity personal multimedia communications systems," *IEICE Transactions on Communications*, vol. E77-B, pp. 1096–1103, September 1994.
- [4] H. Matsuako, S. Sampei, N. Morinaga and Y. Kamio, "Adaptive modulation systems with variable coding rate concatenated code for high quality multi-media communication systems," in *Proceedings of IEEE Vehicular Technology Conference*, pp. 487 – 491, 1996.
- [5] Vincent K. N. Lau and Malcolm D. Macleod, "Variable Rate Adaptive Trellis Coded QAM for High Bandwidth Efficiency Applications in Rayleigh Fading Channels," in *Proceedings of IEEE Vehicular Technology Conference*, pp. 348 – 352, 1998.
- [6] S.G. Chua and A. Goldsmith, "Adaptive Coded Modulation for Fading Channels," *IEEE Transactions on Communications*, vol. 46, pp. 595 – 602, May 1998.
- [7] W.T. Webb and L. Hanzo, *Modern Quadrature Amplitude Modulation : Principles and Applications for Fixed and Wireless Channels*. IEEE Press - John Wiley, 1994.
- [8] J. C. Cheung, *Adaptive Equalisers for Wideband TDMA Mobile Radio*. PhD thesis, University of Southampton, 1991.
- [9] C. Berrou, A. Glavieux and P. Thitimajshima, "Near Shannon Limit Error-Correcting Coding and Decoding : Turbo Codes," in *Proceedings, IEEE International Conference on Communications*, pp. 1064–1070, 1993.
- [10] Joachim Hagenauer, Elke Offer and Lutz Papke, "Iterative Decoding of Binary Block and Convolutional Codes," *IEEE Transactions on Information Theory*, vol. 42, pp. 429–445, March 1996.
- [11] Patrick Robertson, Emmanuelle Villebrum and Peter Hoeher, "A Comparison of Optimal and Sub-Optimal MAP Decoding Algorithms Operating in Log Domain," in *Proceedings of the International Conference on Communications*, pp. 1009–1013, June 1995.
- [12] Office for Official Publications of the European Communities, Luxembourg, *COST 207: Digital land mobile radio communications, final report*, 1989.
- [13] A. Klein, R. Pirhonen, J. Sköld and R. Suoranta, "FRAMES Multiple Access Mode 1 - Wideband TDMA with and without spreading," in *Proceedings of PIMRC'97*, pp. 37–41, 1997.
- [14] J.M. Torrance and L. Hanzo, "Optimization of switching levels for adaptive modulation in a slow Rayleigh fading channel," *IEE Electronics Letters*, pp. 1167 – 1169, June 1996.
- [15] M. K. Simon, J. K. Omura, R. A. Scholtz and B. K. Levitt *Spread Spectrum Communications Handbook*. MacGraw Hill, 1994.